Biosupercapacitors Hot Paper

International Edition: DOI: 10.1002/anie.201607144
German Edition: DOI: 10.1002/ange.201607144

A Nernstian Biosupercapacitor

Dmitry Pankratov, Felipe Conzuelo, Piyanut Pinyou, Sabine Alsaoub, Wolfgang Schuhmann, and Sergey Shleev**

Abstract: *We propose the very first "Nernstian biosupercapacitor", a biodevice based on only one redox polymer: poly(vinyl imidazole-co-allylamine)[Os(bpy)$_2$Cl], and two biocatalysts. At the bioanode PQQ-dependent glucose dehydrogenase reduces the Os^{3+} moieties at the polymer to Os^{2+} shifting the Nernst potential of the Os^{3+}/Os^{2+} redox couple to negative values. Concomitantly, at the biocathode the reduction of O_2 by means of bilirubin oxidase embedded in the same redox polymer leads to the oxidation of Os^{2+} to Os^{3+} shifting the Nernst potential to higher values. Despite the use of just one redox polymer an open circuit voltage of more than 0.45 V was obtained during charging and the charge is stored in the redox polymer at both the bioanode and the biocathode. By connecting both electrodes via a predefined resistor a high power density is obtained for a short time exceeding the steady state power of a corresponding biofuel cell by a factor of 8.*

Realization of efficient electricity generation with minimal loss during storage of the electrical energy is one of the main challenges currently faced by society.[1] Since generation and storage of electrical energy are commonly separated, the overall efficiency is low, increasing not only the monetary but also the environmental costs of electric energy and preventing practical realization of miniature, lightweight, self-powered, and wireless devices.[2] While the recently proposed charge-storing biofuel cells or, in other words, self-charging biosupercapacitors, have the potential to address these problems, only a few supercapacitor/biofuel cell hybrids have been described.[3] Perhaps surprising in light of decades worth of biofuel cell research and development that has been carried out, the study of biomaterials for supercapacitor applications was initiated only seven years ago, resulting in just a few reports.[3,4]

The fundamental concept of a Nernstian biosupercapacitor was demonstrated in 2012 by Malvankar and co-workers using a half-cell, which was able to store electrical charges in the cytochrome C network of a bacterial biofilm.[4b] Herein we demonstrate a complete functional biodevice, specifically, a novel type of charge-storing biofuel cell (BFC), which is based on an Os-complex-modified redox polymer, namely poly(vinyl imidazole-*co*-allylamine)[Os(bpy)$_2$Cl] (**Os-P**). Despite the use of Os-complex-modified hydrogel/oxidoreductase conjugates for the construction of a variety of bioelectronic devices,[5] including high-power BFCs[6] and sensitive and selective biosensors,[7] this is the very first attempt to exploit an Os-complex-modified redox polymer for the design of a self-charging biosupercapacitor. The resulting biodevice is highly capacitive, lightweight, robust, and it also has a unique design feature: it uses only one redox hydrogel for the bioanode and the biocathode.

Conventionally, BFCs based on mediated electron transfer employing redox hydrogels use two different redox polymers with the aim of optimally adapting the redox potentials of the polymers to the redox potentials of the prosthetic groups of the enzymes used. The redox potentials of the redox polymers in turn define the open circuit voltage (OCV) of the BFC and the power is limited by the current provided by the limiting electrode. As far as we are aware, there are no reports concerning BFCs based on the same redox mediator used simultaneously for the bioanode and the biocathode. Evidently, under continuous operation this would lead to a negligible OCV and power density. Herein, we present such a device which we name a "Nernstian biosupercapacitor" (Nernstian BSC). The bioanode oxidizes glucose as fuel and is based on PQQ-dependent glucose dehydrogenase (GDh) entrapped within an **Os-P** film (GDh-Os-P), while the biocathode reduces oxygen using bilirubin oxidase entrapped in the same redox polymer (BOx-Os-P; Figure 1 a). Despite the use of one and the same redox mediator on both cathodic and anodic sides, we realize a powerful biodevice, able to turn on an e-ink based macro-scale display, similar to those widely used in personal electronics applications (Supporting Information Video S1).

The OCV of the complete biodevice as well as the half-cell potentials of the bioanode and biocathode are governed by the $a_{Os^{3+}}/a_{Os^{2+}}$ ratio as derived from the Nernst equation [Eq. (1)], which in turn can be used to relate the numerical values of the electric potential change to the activity change.

$$E = E^0 + (RT/nF)\ln(a_{Ox}/a_{Red}) \quad (1)$$

[*] D. Pankratov, Prof. Dr. S. Shleev
Biomedical Science, Faculty of Health and Society
Malmö University
Södra Förstadsgatan 101, 20506 Malmö (Sweden)
E-mail: sergey.shleev@mah.se
D. Pankratov, Prof. Dr. S. Shleev
Kurchatov's Complex of NBICS-technologies, National Research Center "Kurchatov Institute"
Akademika Kurchatova Sq. 1, 123 182 Moscow (Russia)
Dr. F. Conzuelo, Dr. P. Pinyou, S. Alsaoub, Prof. Dr. W. Schuhmann
Analytical Chemistry—Center for Electrochemical Sciences (CES)
Ruhr-Universität Bochum
Universitätsstrasse 150, 44780 Bochum (Germany)
E-mail: wolfgang.schuhmann@rub.de
Supporting information and the ORCID identification number(s) for the author(s) of this article can be found under http://dx.doi.org/10.1002/anie.201607144.

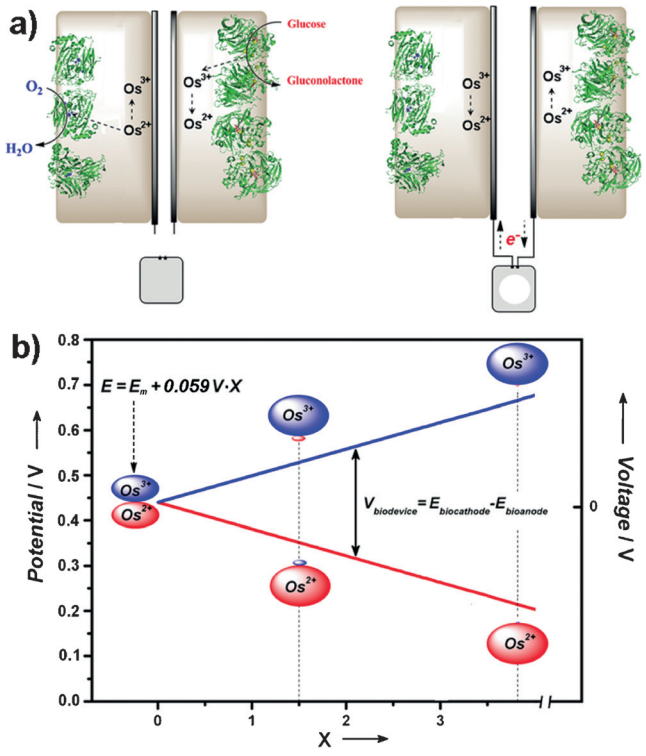

Figure 1. a) Schematic representation of poly(vinyl imidazole-*co*-allylamine)[Os(bpy)$_2$Cl]-based Nernstian BSC during charging (left) and discharging (right). The structures of the enzymes glucose dehydrogenase (GDh) and bilirubin oxidase (BOx) are shown on the right and left sides of the biodevice, respectively, visualized using the crystal structures of the proteins (PDB 2XLL for BOx and 1C9U for GDh). b) Dependence of redox potentials of a biocathode (blue line) and a bioanode (red line) on X according to the Nernst equation [Eq. (1)], where $x = |\log(a_{Os^{3+}}/a_{Os^{2+}})|$. During the redox transformation the overall capacitance of the electrodes (total area of blue and red ellipses) remains constant, while the $a_{Os^{3+}}/a_{Os^{2+}}$ ratio changes during electrode charging and discharging leading to the related change in the voltage difference between bioanode and biocathode.

Where, E is the electrode potential, E^0 is the standard redox potential, a_{Ox} and a_{Red} are activities of oxidized and reduced forms, respectively.

The principle of operation of the Nernstian BSC is based on establishing an activity gradient of a single redox mediator species, that is, the polymer-bound Os complexes. The formation of the activity gradient is driven by enzymatically catalyzed glucose oxidation at the bioanode leading to the concomitant formation of Os^{2+}, and by enzymatically catalyzed reduction of O_2 at the biocathode leading to the formation of Os^{3+} (Figure 1a, left). The charge is stored as a difference in the activity ratio of $a_{Os^{3+}}/a_{Os^{2+}}$ in the volume of the redox polymer on the bioanode and the biocathode. This activity gradient abates when the biodevice is discharged (Figure 1a, right). During the self-charging process, the potentials of the bioelectrodes change according to the Nernst equation, starting from the midpoint (equilibrium) redox potential of the Os-complex-modified redox polymer (E_m) and progressing to non-equilibrium states (Figure 1b), reverting back to the E_m when the Nernstian BSC is fully discharged.

From an existing library of Os-complex-modified hydrogels, we have selected a suitable polymer, **Os-P** (for selection details as well as the characterization of the polymer see Supporting Information, Section 1), which has been previously used showing fast electron transfer (ET) by electron hopping and sufficient long-term stability.[8] In contrast to the selection of suitable redox polymers for conventional BFCs, the redox potential of the redox polymer for a Nernstian BSC should be between those of the prosthetic groups of the enzymes used for the bioanode and biocathode reactions. This guarantees a high driving force for the ET between the polymer-bound redox mediator and the enzymes. In addition, the polymer film should be heavily loaded with redox mediators and also have a substantial thickness to ensure high pseudocapacitance. Moreover, the redox mediator should show a low affinity towards molecular oxygen to avoid parasitic O_2 electroreduction at the bioanode.

We fabricated, characterized, and optimized separate capacitive bioelectrodes (Supporting Information Section 3). The optimized bioanodes and biocathodes provided maximal bioelectrocatalytic current densities of 55 $\mu A\,cm^{-2}$ and 85 $\mu A\,cm^{-2}$, respectively, being simultaneously highly capacitive with a capacitance density equal to 147 $mF\,cm^{-2}$, where pseudo and double-layer capacitances are 114 $mF\,cm^{-2}$ and 33 $mF\,cm^{-2}$, respectively (Figure 2a). Note that the midpoint potentials of GDh-Os-P and BOx-Os-P conjugates are very close to the redox potential of **Os-P** (0.44 V), as well as to each other, that is, 0.45 and 0.44 V, respectively (cf. dashed curves in Figures S1 and S2). The two bioelectrodes were combined to form a Nernstian BSC, and detailed electrochemical characterization in the presence and absence of the enzyme substrates, glucose and O_2, was carried out. In contrast to the methodology used previously,[3a,b,d] we monitored the OCV of the biodevice as well as the open-circuit potentials (OCPs) of the bioanode and biocathode separately (herein and below all potentials are given vs. NHE), during both self-charging and external discharging (Figure 2b, Supporting Information Section 2).

Average specific charge and power densities were derived (1700 $mC\,g^{-1}$ and 3.9 $mW\,g^{-1}$, respectively) from discharge curves of the biodevice (Figure 2b and Figure 3a, as well as Figures S2 and S3). 3.9 $mW\,g^{-1}$ power density is slightly higher than those reported previously for biodevices based on electrodes made of combinations of bioelectrocatalytic and charge-storing components (3.8 and 1.8 $mW\,g^{-1}$, as calculated from experimental results presented in Refs. [3a] and [3d], respectively). However, the specific charge density attained in the Nernstian BSC was dramatically higher, at 1700 $mC\,g^{-1}$ versus 0.06 and 48 $mC\,g^{-1}$ as derived from Ref. [3a,d]. Moreover, the weight of the proposed Nernstian BSC is comparatively low with only 0.5 mg versus 550 and 47 mg for the devices proposed in Ref. [3a,d]. One of the most important parameters determining the ultimate usability of a bioelectronic device is its stability. We addressed this issue by performing experiments to evaluate the short-term and long-term operational stability as well as storage stability (Supporting Information, Section 4). Stability tests were carried out not only using the complete biodevice (Figure 3a),

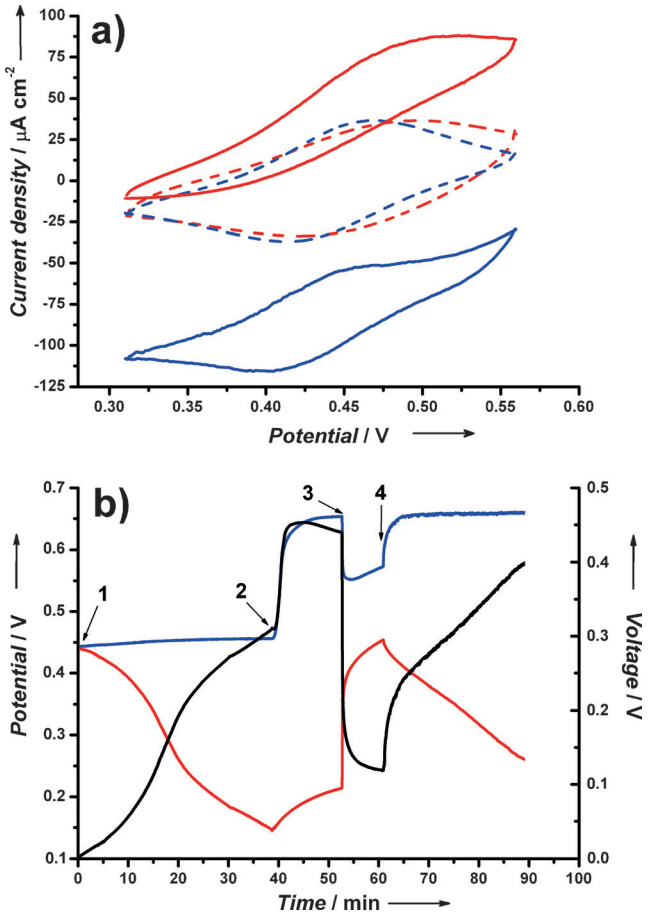

Figure 2. a) Cyclic voltammograms of biocathodes (blue traces) and bioanodes (red traces) in Ar-saturated PBS (dashed traces) and O_2-saturated PBS containing 20 mM glucose (solid traces); scan rate: 0.2 mV s^{-1}. b) Charge/discharge traces of the Nernstian BSC in PBS: 1. addition of 20 mM glucose; 2. bubbling of O_2; 3. discharging at a constant load of 10 kΩ; and 4. disengaging the load. Red trace: OCP of the bioanode; blue trace: OCP of the biocathode; black trace: OCV of the Nernstian BSC.

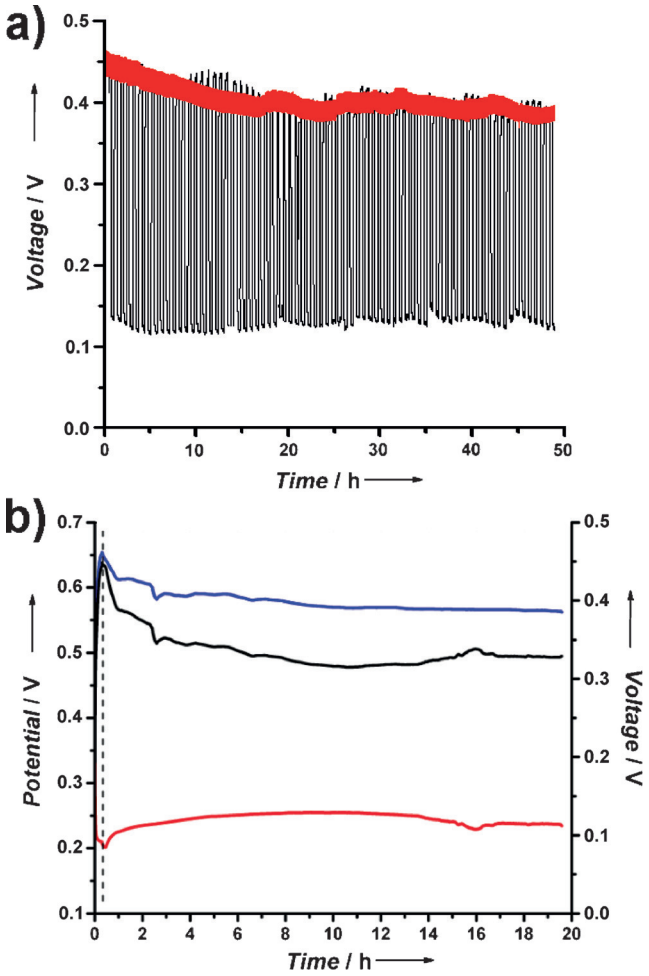

Figure 3. a) Operational stability tests of the Nernstian BSC in long-term (black trace) and short-term (red trace) pulse modes in O_2-saturated PBS containing 20 mM glucose. b) Charge-storing stability of separate bioelectrodes and complete Nernstian BSC. A fully charged Nernstian BSC was rinsed with water and transferred into Ar-saturated PBS (20 min, dashed line). Red trace: OCP of bioanode; blue trace: OCP of biocathode; black trace: OCV of Nernstian BSC.

but also using the bioanode and biocathode separately in extended half-cell tests (Figure S4).

The operational lifetime of the biodevice in both short-term and long-term pulse tests exceeds 48 h (Figure 3a). Moreover, the biodevice displays low leakage currents on both anodic and cathodic sides, losing only 25% of its initial voltage when stored in a substrate-free electrolyte for 20 h (Figure 3b).

Following a recently proposed classification scheme for self-charging biosupercapacitors (double-layer, pseudo, and hybrid)[3c] and taking into account the high pseudo/double-layer capacitance ratio of approximately 3.5 of the bioelectrodes, we consider the proposed Nernstian biodevice to be a pseudobiosupercapacitor. The Nernstian BSC generates electricity by burning bio-fuels (e.g. glucose) with concomitant reduction of O_2 to H_2O utilizing biocatalysts exactly as conventional BFCs do (Figure 1a). However, in contrast to conventional enzymatic BFCs (for a detailed comparison see Supporting Information, Section 5), which can only provide current to an external electrical circuit and do not store electrical energy. Hence, their power is limited in the case of ideal Nernstian systems (Figure 4). The Nernstian BSC can accumulate charges in the anode and cathode due to self-polarization with concomitant change of their potentials in opposite directions, defining the OCV and the maximal initial operating voltage at the end of the charging process according to the Nernst equation (Figure 1b).

The potential difference between the standard redox potentials of the two half-cells of 1.18 V (gluconolactone/glucose, 0.05 V and O_2/H_2O, 1.23 V at pH 0) is a measure of the thermodynamic driving force of the electricity generating process (Figure 4).

The non-turnover signals in Figure 4 for surface-confined redox-active species PDH, Os-P, and BOx, were modelled using Equation (2) (the Nernst equation written in terms of the concentrations of Os-P and the enzymes on the electrode surface), assuming ideal Nernstian behavior of the immobilized redox species and that their adsorption abilities are equal for reduced and oxidised forms.

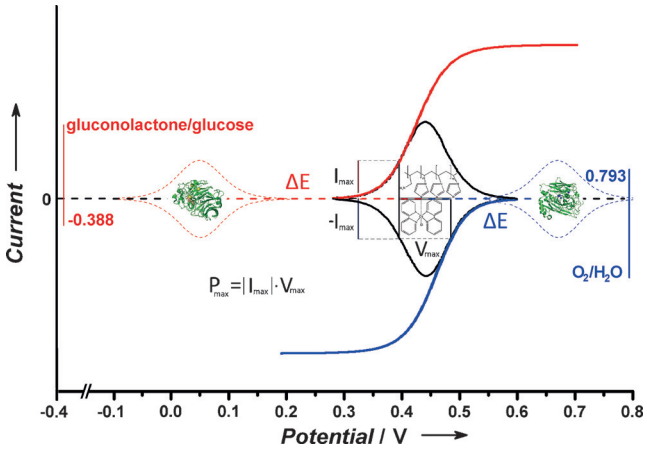

Figure 4. Modelled current–potential curves for surface-confined redox-active species used in the current work. Dotted red and blue cyclic voltammograms: non-turnover Faradaic signals from GDh and BOx, respectively. Solid black voltammogram: poly(vinyl imidazole-*co*-allylamine)[Os(bpy)$_2$Cl] (the polymer structure is shown inside the voltammogram). Solid red and blue linear sweep voltammograms: turnover signals for GDh and BOx incorporated into the polymer in the presence of enzyme substrates, glucose and oxygen, respectively. Vertical red and blue lines: equilibrium redox potentials in PBS of gluconolactone/glucose and O_2/H_2O couples, respectively. Red and blue zero current dashed straight lines: potential differences (ΔE) between redox potentials of the polymer and enzymes.

$$i = \frac{n^2F^2}{RT}\frac{\nu A\Gamma \exp[(nF/RT)(E-E^0)]}{\{1+\exp[(nF/RT)(E-E^0)]\}^2} \quad (2)$$

Where, ν is the potential scan rate (0.1 V s^{-1}), A is the electrode area (0.173 cm^2), Γ is the surface concentration of redox-active species, with $\Gamma_{Os} \approx 2\Gamma_{enzyme}$, and other symbols have their usual meanings.[9] Turnover signals for redox enzymes incorporated into the polymer in the presence of enzyme substrates are plotted using a mathematical model described by Equation SI18 in Ref. [10], assuming that the heterogeneous ET constant is higher than the bioelectrocatalytic constant ($k_{cat}/k_0 = 0.2$), $\alpha = 0.5$, and that onset potentials of bioelectrocataliyc processes differ by 0.15 V from E_m of Os-P (0.44 V). This redox potential is suitable for both enzymes since there is sufficient driving force for the anodic ($\Delta E =$ 0.39 V) and cathodic ($\Delta E = 0.23$ V) bioelectrocatalytic processes (Figure 4). The redox potential of PQQ-sGDh was assumed to be about 0.05 V versus NHE (reported midpoint values for the immobilized enzyme vary between 0 to 0.1 V depending on electrode material, pH value, and type of redox mediator).[11] The redox potential of the first electron acceptor of BOx, the T1 Cu site, is 0.67 V versus NHE.[12]

In our studies the maximal achieved OCV was as high as 0.45 V (Figure 2b, black curve), implying that 99.97 % of the Os complexes were transformed into Os^{2+} and Os^{3+} for the bioanode and biocathode, respectively; $|\log(a_{Os^{3+}}/a_{Os^{2+}})|$ as high as 3.82 (Figure 1b). This high charge-storage efficiency reflects low leakage currents on both anode and cathode since the maximal achievable redox potential of a bioelectrode is determined by the charging/leakage current ratio, that is, the bioelectrode potential is stabilized when self-charging and self-discharging (leakage) processes are in equilibrium. The charging time of the overall biodevice depends on the bioelectrocatalytic activity of the lower-performing and hence limiting electrode versus its capacitance (Supporting Information, Section 2). Thus, for optimization not only capacitances but also bioelectrocatalytic currents should be equal on the anodic and cathodic sides. This is challenging to achieve considering the huge variations in specific activities of anodic and cathodic redox enzymes. In contrast to BFCs, for which optimization can be done simply by adjusting electrode sizes (Supporting Information, Section 5) hence increasing the bioelectrocatalytic current output of a limiting bioelectrode, an ideal Nernstian BSC should have equal bioelectrocatalytic ability and capacitance for both electrodes.

To conclude, we demonstrate proof-of-principle operation of a self-charging Nernstian BSC that is capable of operating as a sustained source of electricity, able to power an e-ink display (Supporting Video S1). Despite the use of just one polymer-bound redox mediator, we realize a highly capacitive, lightweight, and stable biodevice with superior characteristics compared to other BSCs.[3a,d] Considering that all the BFCs reported to date utilize two different redox mediators we anticipate that this work will be a starting point for rethinking the strategies in the design of new, highly functional, but at the same time low-cost and technically undemanding biological electric power sources.

Acknowledgements

This work has been financially supported by the European Commission (PEOPLE-2013-ITN-607793), the Deutsch–Israelische Projektkooperation in the framework of the project "Nanoengineered optoelectronics with biomaterials and bioinspired assemblies", the Cluster of Excellence RESOLV (EXC 1069) funded by the Deutsche Forschungsgemeinschaft (DFG), the Russian Science Foundation (14-14-00530), and the Swedish Research Council (621-2013-6006).

Keywords: bioelectrocatalysis · biofuel cells · Nernstian biosupercapacitor · redox hydrogels

How to cite: *Angew. Chem. Int. Ed.* **2016**, *55*, 15434–15438
Angew. Chem. **2016**, *128*, 15660–15664

[1] a) D. Larcher, J. M. Tarascon, *Nat. Chem.* **2015**, *7*, 19–29; b) M. Bilgili, A. Ozbek, B. Sahin, A. Kahraman, *Renewable Sustainable Energy Rev.* **2015**, *49*, 323–334.
[2] D. Pankratov, P. Falkman, Z. Blum, S. Shleev, *Energy Environ. Sci.* **2014**, *7*, 989–993.
[3] a) C. Agnes, M. Holzinger, A. Le Goff, B. Reuillard, K. Elouarzaki, S. Tingry, S. Cosnier, *Energy Environ. Sci.* **2014**, *7*, 1884–1888; b) D. Pankratov, Z. Blum, S. Shleev, *ChemElectroChem* **2014**, *1*, 1798–1807; c) D. Pankratov, Z. Blum, D. B. Suyatin, V. O. Popov, S. Shleev, *ChemElectroChem* **2014**, *1*, 343–346; d) M. Kizling, S. Draminska, K. Stolarczyk, P. Tammela, Z. Wang, L. Nyholm, R. Bilewicz, *Bioelectrochemistry* **2015**, *106*, 34–40.
[4] a) J. Lee, H. Yi, W.-J. Kim, K. Kang, D. S. Yun, M. S. Strano, G. Ceder, A. M. Belcher, *Science* **2009**, *324*, 1051–1055; b) S. Malvankar Nikhil, T. Mester, T. Tuominen Mark, R. Lovley Derek, *ChemPhysChem* **2012**, *13*, 463–468.

[5] a) S. Boland, P. Kavanagh, D. Leech, *ECS Trans.* **2008**, *13*, 77 – 87; b) P. Pinyou, A. Ruff, S. Poeller, S. Ma, R. Ludwig, W. Schuhmann, *Chem. Eur. J.* **2016**, *22*, 5319 – 5326.
[6] D. Leech, P. Kavanagh, W. Schuhmann, *Electrochim. Acta* **2012**, *84*, 223 – 234.
[7] X. Feng, K. Zhang, M. A. Hempenius, G. J. Vancso, *RSC Adv.* **2015**, *5*, 106355 – 106376.
[8] a) A. Badura, D. Guschin, B. Esper, T. Kothe, S. Neugebauer, W. Schuhmann, M. Roegner, *Electroanalysis* **2008**, *20*, 1043 – 1047; b) A. Badura, D. Guschin, T. Kothe, M. J. Kopczak, W. Schuhmann, M. Roegner, *Energy Environ. Sci.* **2011**, *4*, 2435 – 2440; c) T. Kothe, S. Poeller, F. Zhao, P. Fortgang, M. Roegner, W. Schuhmann, N. Plumere, *Chem. Eur. J.* **2014**, *20*, 11029 – 11034.
[9] V. Climent, J. Zhang, E. P. Friis, L. H. Oestergaard, J. Ulstrup, *J. Phys. Chem. C* **2012**, *116*, 1232 – 1243.
[10] A. J. Bard, L. R. Faulkner, *Electrochemical Methods: Fundamentals and Applications*, Wiley, New York, **1980**, p. 718.
[11] V. Flexer, N. Mano, *Anal. Chem.* **2014**, *86*, 2465 – 2473.
[12] A. Christenson, S. Shleev, N. Mano, A. Heller, L. Gorton, *Biochim. Biophys. Acta Bioenerg.* **2006**, *1757*, 1634 – 1641.

Received: July 23, 2016
Revised: September 1, 2016
Published online: November 2, 2016

